NUMERICAL ANALYSIS OF MEDIUM COMPRESSION AND LOSSES IN FILTRATION AREA IN PLEATED CARTRIDGE MEMBRANE FILTERS

A.N. Waghode, N.S.Hanspal, R.J. Wakeman,V. Nassehi

Advanced Separation Technologies Group
Department of Chemical Engineering, Loughborough University,
Loughborough, Leicestershire, LE11 3TU, UK
Tel: + 44 (0) 1509222533
Fax: +44 (0) 1509223923

Abstract

A computer model has been developed to simulate the fluid flow in pleated filter cartridges. This model has been used to evaluate the performance and design of pleated cartridge membrane filters. The effects of medium compression, pleat deformation and pleat crowding are analysed. At higher flow rates, due to the fluid pressure exerted the medium deforms which leads to a reduction in the material permeability. Further, pleating and bending leads to a loss in effective filtration area. The combined effects of compression and reduction in filtration area cause deviations from Darcy's law. To interpret such deviations, permeability models based on the data obtained from the flat sheets of the filter material used in cartridge fabrication have been developed. The incorporation of the permeability model within the main hydrodynamic model determines the percentage losses in filtration area, percentage medium compression and the pressure drop across the filters. Results in this paper are presented for a fibre glass medium. The simulated results have been compared against experimental data for purposes of model validation. The developed simulation tool offers a robust, cost-effective and user friendly design and analysis tool for pleated cartridge membrane filters, which can be easily used by engineers in industry.

Keywords: Medium compression, Permeability, Pleat crowding, Filtration area, Darcy's law, Cartridge Filters

INTRODUCTION

Due to the high surface area offered in a smaller occupied volume, pleated cartridge filters are the first choice of preference in many industrial applications. There has been an increasing interest in the design of filter cartridges that have a lower environmental impact through their use and disposal due to, for example, their reduced weight and alternative materials of construction and reduced disposal costs. Though the present study focuses on a deadend filtration process, the approach is generic and can be extended to develop both deadend and cross flow filtration (Hanspal *et al*, 2004) models for a variety of applications found in automotive, water treatment, and pharmaceutical industries.

Strategies employed by engineers for modelling flow within filter cartridges are commonly based on simplifications in the geometry or flow regime characteristics. Wakeman and Harris (1993) attempted a methodology for modelling pleated cartridges, in order to predict magnitude and direction of fluid and particle velocities, the pressure distribution, the permeability of the filter cake or a measure of particle deposition. If cake starts building during filtration, the volume of the flow region upstream of the pleat will change, posing extra complexity to the problem. It was assumed that there was no formation of cake, which is the practical case when filtering low concentrations of smaller particles. The model was developed specifically for "star" pleat configurations, which were considered to have symmetry in radial direction, therefore requiring only half of the pleat to be modelled.

Chen *et al* (1995) developed a numerical model to optimise the design of pleated filter panels. The pleats are taken to be simple rectangles. In addition, uniform velocity profiles are assumed in the upstream pleat channel and sinusoidal in downstream channel. It is further assumed that the fluid penetrates in the porous medium only at the top and bottom regions of the pleat, any penetration along the length of the pleat is negligible. The free flow is modelled by Stokes equations while the porous flow is modelled by Darcy-Lapwood-Brinkman equation to compensate for the simplified velocity profiles.

More recently, Oxarango *et al* (2004) developed a one-dimensional model to determine laminar flow of a fluid in porous channels with wall suction or injection. They extended their approach to pleated filters by a two-dimensional model using a unit element of the pleated filter with periodic boundary conditions. The pleats considered in their work are again of rectangular geometry and the intrusion of the fluid in porous media is assumed to be unidirectional. However, such simplifications reduce the applicability of these models to realistic industrial situations where the flow geometry is usually complex and flow regime is multi-dimensional and highly non-uniform.

In the present work, the hydrodynamic model developed by the authors has been tested and validated for industrial situations. A typical cartridge assembly used can be seen in Figure 1. The cartridge filter assembly consists of three distinct flow regions. The cross sectional view for the outermost free flow region between the outer metal casing and porous cartridge, the porous flow region (the filter medium itself) and the inner free flow region (the core) has been presented in Figure 2. The bulk of the pressure drop occurs within the porous filter medium and hence the modelling is primarily based on developing a porous flow model (Hanspal *et al*, 2004; Waghode *et al*, 2004; Ruziwa *et al*, 2003, 2004).

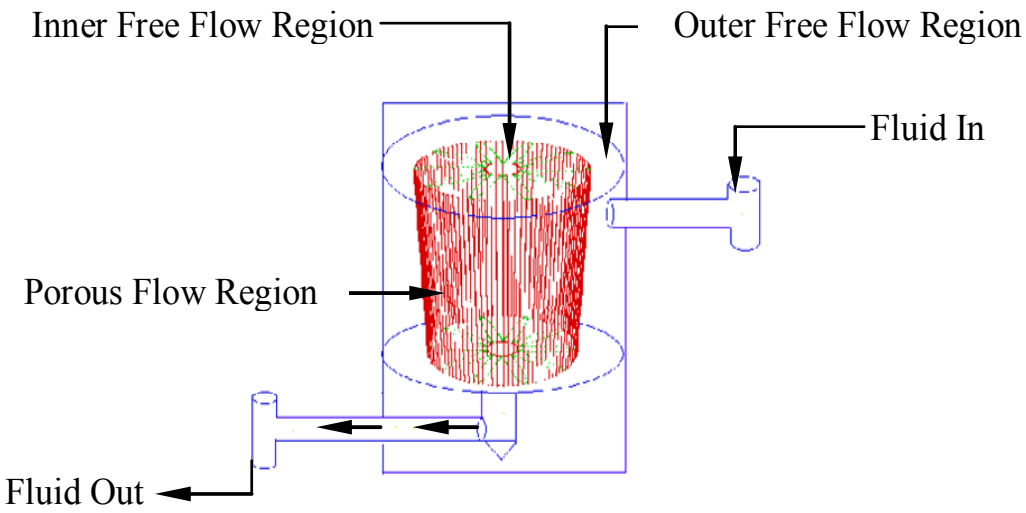

Figure 1. Cartridge Filter Assembly

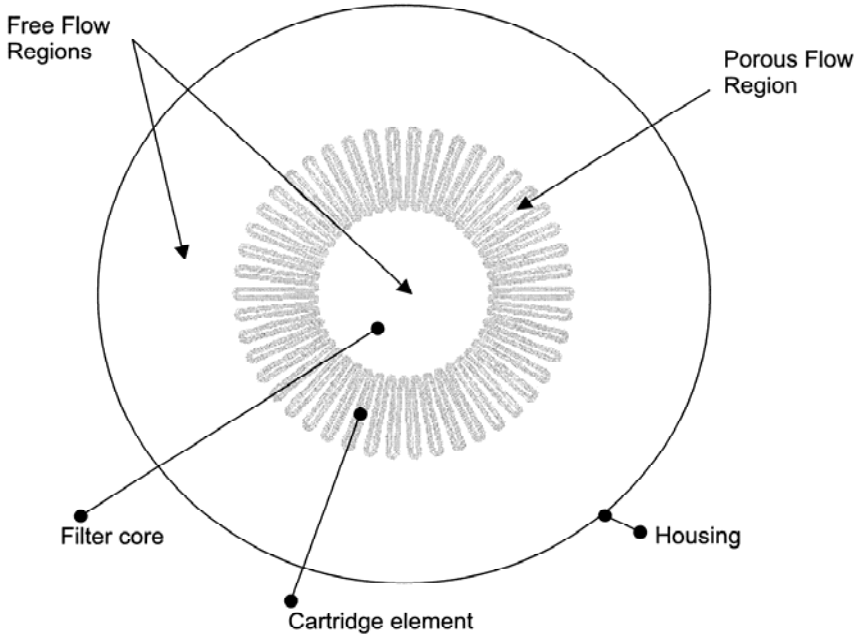

Figure 2:Cross-section of a pleated cartridge showing the three principal flow zones to be modelled: 1. the region inside the housing and upstream of the medium; 2. the filter medium, and 3. the region downstream of the medium in the filter core.

In the preliminary studies by the authors, model complexities such as changes in permeability, compression of pleats and losses in filtration area as a result of pleat crowding effects have been ignored. These effects can generally be seen at higher rates of fluid flow, or when the fluid viscosity is high, or when the cartridge contains a large number of pleats. The laminar, incompressible and non-inertial flow of a viscous fluid through a permeable medium with low permeability is governed by Darcy's law. For flow of a clear fluid through a fixed porous medium, the relationship between the pressure gradient and the velocity is linear. However, the pressure drop across the permeable medium can deviate from the Darcy's equation in cases when there is an appreciable compression of the permeable medium or when changes in filtration area occur. The non-ideal flow behaviour through the porous medium is a result of a continuous force exerted by the fluid on the filtering medium, which leads to medium compression resulting in a reduction of its permeability. The present study is an attempt directed towards predicting accurate values of percentage losses in filtration area, percentage medium compression and the pressure drop which will assist in designing new cartridge filter elements. Experimental data obtained for the fibre glass media serves the basis for model validation.

MATHEMATICAL MODEL

The overall mathematical model for simulating the fluid flow within pleated cartridge consists of a hydrodynamic model, a constitutive relationship, a permeability model and a medium compression and apparent loss in filtration area model. In the development of the model we consider the following assumptions;

1. The flow regime is creeping (near zero Reynolds number stokes flow);
2. The fluid is incompressible;
3. Gravitational forces are negligible;
4. The hydraulic fluid used are shear thickening generalised Newtonian fluids.

Hydrodynamic model

The transient flow hydrodynamics in the porous flow regime are described by the momentum and mass conservation equations, also commonly known as the Darcy and the Continuity equations. In 2-D cartesian coordinate systems these equations can be represented by

(a) The Darcy equation

$$\begin{cases} \rho\dfrac{\partial v_x}{\partial t}+\dfrac{\eta}{K_x}v_x+\dfrac{\partial p}{\partial x}=0 \\ \rho\dfrac{\partial v_y}{\partial t}+\dfrac{\eta}{K_y}v_y+\dfrac{\partial p}{\partial y}=0 \end{cases} \tag{1}$$

(b) The Continuity equation

$$\frac{1}{\rho c_s^2}\frac{\partial p}{\partial t}+\frac{\partial v_x}{\partial x}+\frac{\partial v_y}{\partial y}=0 \tag{2}$$

where ρ is the fluid density, v_x and v_y are the components of the velocity vector, t is the time variable, η is the fluid viscosity, K_x and K_y are the permeability components, p is the pressure and c_s is the speed of sound in the fluid.

Equation (2) is a slightly perturbed form of the continuity equation, which has been used in the current model to satisfy the Ladyzhenskaya-Babuska-Brezzi stability condition (Nassehi, 2002).

Constitutive relationship

As the filtration operation progress, the viscosity of the hydraulic fluid cotinuously changes. The fluid is assumed to behave as a generalized Newtonian fluid and its viscosity is updated through iterative loops in the solution algorithm using the power law model,

(c) Power Law Model

$$\eta = \eta_0 \left(\dot{\gamma}\right)^{n-1} \tag{3}$$

The shear rate is calculated as

$$\dot{\gamma} = \left[2\left(\frac{\partial v_x}{\partial x}\right)^2 + \left(\frac{\partial v_x}{\partial y} + \frac{\partial v_y}{\partial x}\right)^2 + 2\left(\frac{\partial v_y}{\partial y}\right)^2 \right]^{\frac{1}{2}} \tag{4}$$

where, η is the fluid viscosity, η_0 is the viscosity of the fluid at zero shear, $\dot{\gamma}$ is the shear rate and n is the power law index which for a shear thickening fluid is more than 1.

Permeability Model

The alteration in the permeability value occurs as a result of medium compression which is in turn attributed to medium folding and hydrodynamic drag exerted by the flowing fluid on the surface of the medium. The permeability models are media specific and can be determined by carrying out a detailed analysis of flat sheet experimental data (Wakeman *et al*, 2004). In these models, the permeability of the medium can be represented as a function of pressure drop through the porous domain.

The flat sheet fibre glass medium with thickness 590 μm at 20 kPa, pore size 2.7 μm, basis weight 92 g.m^{-2} was analysed to develop the permeability model. The hydraulic fluid used in the experiments was an oil with a density of 880 kg.m^{-3}, an average kinematic viscosity of 63 cSt, and a power law index of 1.0. The filtering area of the flat sheet used for carrying out the experiments was 28.3 cm^2. The developed model can be mathematically represented as,

$$\left.\begin{aligned} K = K_x = K_y &= 1.97\times10^{-12}\ \text{m}^2 \text{ when } \Delta p < 1.13\times10^5\ \text{Pa} \\ K = K_x = K_y &= 3.26\times10^{-11}\Delta p^{-0.2397}\ \text{m}^2 \text{ when } 1.13\times10^5 < \Delta p < 10.8\times10^5\ \text{Pa} \\ K = K_x = K_y &= 1.04\times10^{-12}\ \text{m}^2 \text{ when } \Delta p > 10.8\times10^5\ \text{Pa} \end{aligned}\right\} \tag{5}$$

The variation of permeability with pressure for glass fibre is shown in Figure 3.

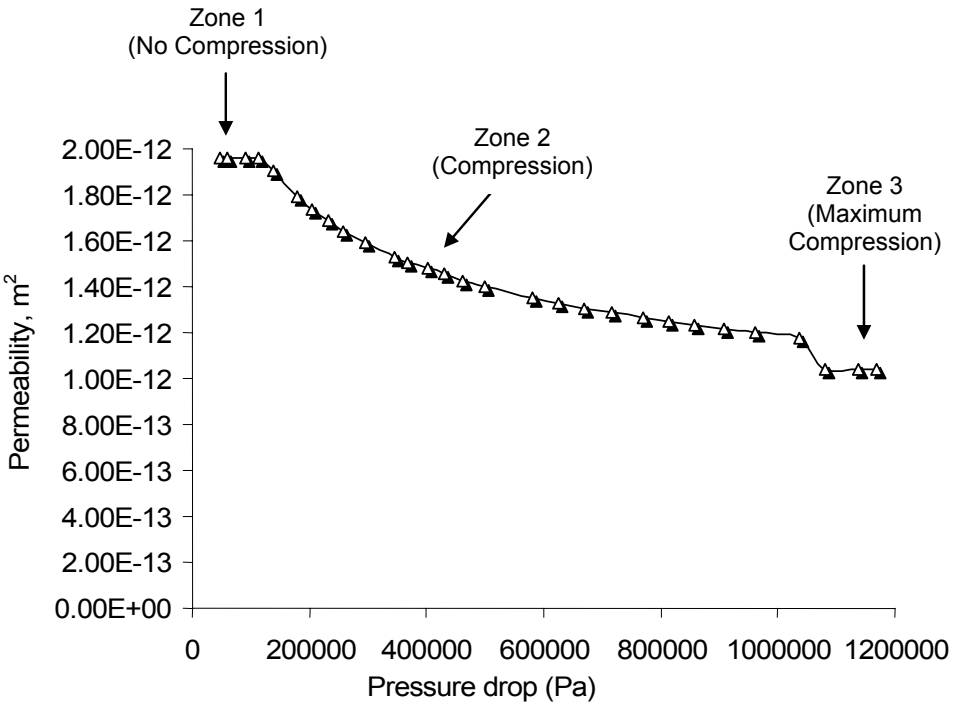

Figure 3: Permeability – pressure drop model for the fibre glass medium

Medium compression and apparent loss in filtration area model

The reasons for medium compression have been listed in the previous section, however apparent losses in filtering area occur as a result of geometric effects. The most prominent geometric effects are the pleat crowding and pleat deformation. The former occurs when there are too many pleats in a single cartridge whereas the later occurs as a result of excessive height of the pleats and longer cartridge designs (Wakeman *et al*, 2004).

The degree of compression or the percentage compression for a given filter cartridge element under given flow conditions can be calculated using,

$$\% \text{ Compression} = \frac{K - K_c}{K} 100 \tag{7}$$

where, K_c is the permeability of the compressed medium (given by equations 5), and K is the permeability of the medium without no compression (represented by Zone 1, Figure 3).

Apparent losses of filtration area can be estimated using the pressure drop across the cartridge obtained from experiments, p_{exp}. The percentage loss in filtration area can be evaluated using

$$\% \text{ Loss of Area} = \frac{p_{exp} - p_c}{p_c} 100 \tag{8}$$

where, p_c is the simulated pressure drop across the cartridge obtained using the compressed medium permeability, K_c.

MODELLING STRATEGY

An iterative finite element solution scheme was developed through the derivation of appropriate system of transient working equations for the hydrodynamic model. The final working equations incorporated in the main solution algorithm have been presented elsewhere (Hanspal *et al*,2004; Ruziwa *et al*,2004). A standard Galerkin weighted residual finite element method was employed taking in account the complex geometry of the cartridge. C^0 continuous nine-noded biquadratic Lagrangian elements were used for the domain discretisation and approximation of the field variables i.e. velocities and pressure. The temporal discretisation was based on a Euler time-stepping method. The incorporation of the permeability model within the main hydrodynamic model yields the simulated pressure drop values. The compression and loss in apparent filtration area model when embedded, accounts for degrees of compression, losses in filtering area and model validation.

COMPUTATIONAL RESULTS AND DISCUSSIONS

Two different types of filter element geometries i.e. (ID 1 and ID 2) were used during for experiments and simulations The geometrical and physical parameters for both the filters have been presented in Table 1. The elements just differ in terms of total number of pleats and all the other geometrical parameters, fluid flow physical properties are the same. For model validation experimental cartridge permeation test data has been used.

Table 1: Geometric and physical parameters for experiments and simulations for two different filter element geometries

Physical property	Filter ID 1	Filter ID 2
Filter Media	Fibre glass (β = 3μm >200) with metal square mesh (aperture 440 μm) support	Fibre glass (β = 3μm >200) with metal square mesh (aperture 440 μm) support
Fluid density	880 $kg.m^{-3}$	880 $kg.m^{-3}$
Fluid viscosity	70 cSt	70 cSt
Power law index	1.0	1.0
Total number of pleats	70	75
Length of the filter element	211.5 mm	211.5 mm
Height of the pleat	24.5 mm	24.5 mm
Diameter of the core	59.0 mm	59.0 mm
Nominal filter area	0.681 m^2	0.729 m^2

The main processor consists of a 2-D finite element program that has been developed in FORTRAN. The computational mesh used in the calculations consists of a repetitive unit of the cartridge element (shown in Figure 4), whose simulation has been shown to be equivalent to the modelling of the whole filter domain (Ruziwa *et al*, 2003). The simulations on the repetitive unit reduces the computational time. The dimensions of the repetitive units have been taken from the actual pleated cartridge filter geometry used in the experimentations. The computational mesh in figure 5 consists of 2400 elements and 10101 nodes respectively.

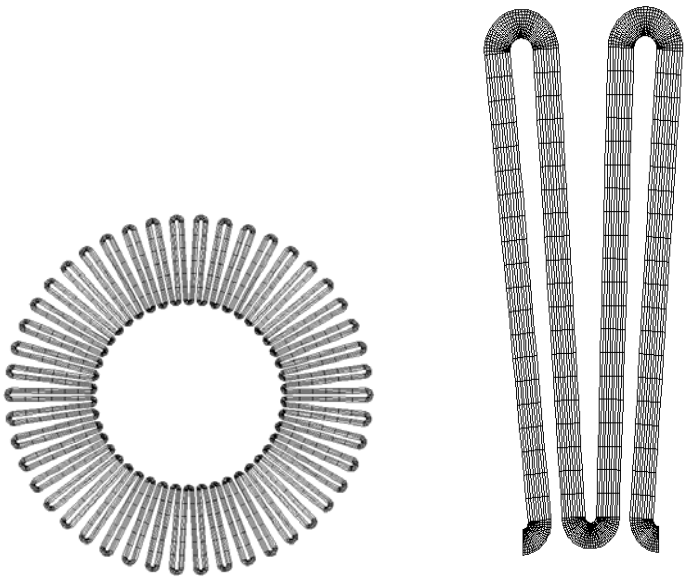

Figure 4: Finite element meshes for the whole filter domain (left) and the repetitive unit (right); comparisons of calculated pressure losses over different parts of the pleat in the repetitive unit are comparable with pressure losses over the same parts of the pleat in the whole domain. Use of the repetitive unit speeds up computation and is used for the simulations in this paper

Results for both the filters have been presented in Tables 2(a), 2(b) and 3(a), 3(b) respectively. In Tables 2(a) and 3(a) simulated pressure drops p_{c+a} for ID 1 and ID 2 have been presented which have been calculated after both the compression and apparent losses in filtration area have been incorporated in the main hydrodynamic model. The detailed analysis for incorporation of compression and loss in area effects whilst carrying out the simulations has been reported elsewhere (Wakeman *et al*, 2004). In Figures 5 and 6, the deviations from the ideal Darcy behaviour can be seen for ID 1 and ID 2 due to compression and loss in filtration area effects. The first curve represents experimental pressure drops. The second curve in Figures 5 and 6 represent a linear flow rate versus pressure drop relationship (i.e. Darcy's law), without inclusion of any of the effects listed above. The third curve indicates the flow rate versus pressure drop relationship once compression (i.e. reduction in permeability due to compression) has been accounted. The fourth curve corresponds to the non-linear flow rate versus pressure drop relationship after the incorporation of the listed effects. The simulated pressure drop values p_{c+a} on the fourth curve which include compression and loss in area effects, agree closely with the experimental test data p_{exp} (values on the first curve) thus validating our filter model. It is also seen in Figure 7, that as the number of pleats increases from 70 (ID 1) to 75 (ID 2) simulated percentage losses in filtration area increase from the range of 71-75% to 83-85% illustrating the pleat crowding effect. The area losses suggest a possible reduction in the amount of material required for filter fabrication. This would enhance the economy of cartridge manufacturing process and also the operational economy in many filtration applications (i.e. aeronautics) where the weight of the filter element is considered to be crucial.

Table 2(a): Comparison between the experimental and simulated pressure drops : Filter ID 1

Experimental values			Calculated data			
Flow rate ($l\ min^{-1}$)	**Face velocity** ($m\ s^{-1}$)	**Pressure drop** p_{exp} (bar)	**Pressure drop with compression** p_c (bar)	**% loss of area**	**Velocity corrected for loss of area** ($m\ s^{-1}$)	**Pressure drop allowing for compression and loss of area** p_{c+a} (bar)
50	0.0024	3.79	0.936	75.30	0.0099	3.790
100	0.0037	5.84	1.513	74.09	0.0142	5.840
150	0.0049	8.39	2.168	74.16	0.0189	8.390
200	0.0061	10.81	3.215	70.26	0.0206	10.811
250	0.0073	13.29	3.858	70.97	0.0253	13.291
300	0.0087	15.85	4.501	71.60	0.0302	15.852
350	0.0098	18.30	5.221	71.47	0.0343	18.300

Table 2(b): Calculated percentage compression and loss in area: Filter ID 1

Flow rate ($l.min^{-1}$)	**% Compression**	**% Loss of area**
50	23.86	75.30
100	31.36	74.09
150	37.07	74.16
200	46.95	70.26
250	46.95	70.97
300	46.95	71.60
350	46.95	71.47

Table 3(a): Comparison between the experimental and simulated pressure drops : Filter ID 2

Experimental values			Calculated data			
Flow rate ($l.min^{-1}$)	**Face velocity** ($m.s^{-1}$)	**Pressure drop** p_{exp} (bar)	**Pressure drop with compression** p_c (bar)	**% Loss of area**	**Velocity corrected for loss of area** ($m.s^{-1}$)	**Pressure drop allowing for compression and loss of area** p_{c+a} (bar)
100	0.0023	2.28	0.320	85.98	0.0163	2.280
150	0.0034	3.45	0.514	85.09	0.0230	3.450
200	0.0046	4.98	0.749	84.96	0.0304	4.979
250	0.0057	6.41	0.980	84.72	0.0374	6.409
300	0.0068	7.98	1.222	84.68	0.0447	7.979
350	0.0080	9.65	1.493	84.53	0.0517	9.649
400	0.0091	11.13	1.928	82.68	0.0528	11.130
450	0.0103	12.30	2.168	82.37	0.0583	12.300
500	0.0114	13.97	2.409	82.75	0.0660	13.969
550	0.0126	16.07	2.691	83.25	0.0750	16.070
600	0.0137	17.77	2.975	83.25	0.0818	17.769

Table 3(b): Calculated percentage compression and loss in area: Filter ID 2

Flow rate ($l\ min^{-1}$)	**% Compression**	**% Loss of area**
100	13.99	85.98
150	22.13	85.09
200	28.68	84.96
250	32.87	84.72
300	36.31	84.68
350	39.14	84.53
400	46.95	82.68
450	46.95	82.37
500	46.95	82.75
550	46.95	83.25
600	46.95	83.25

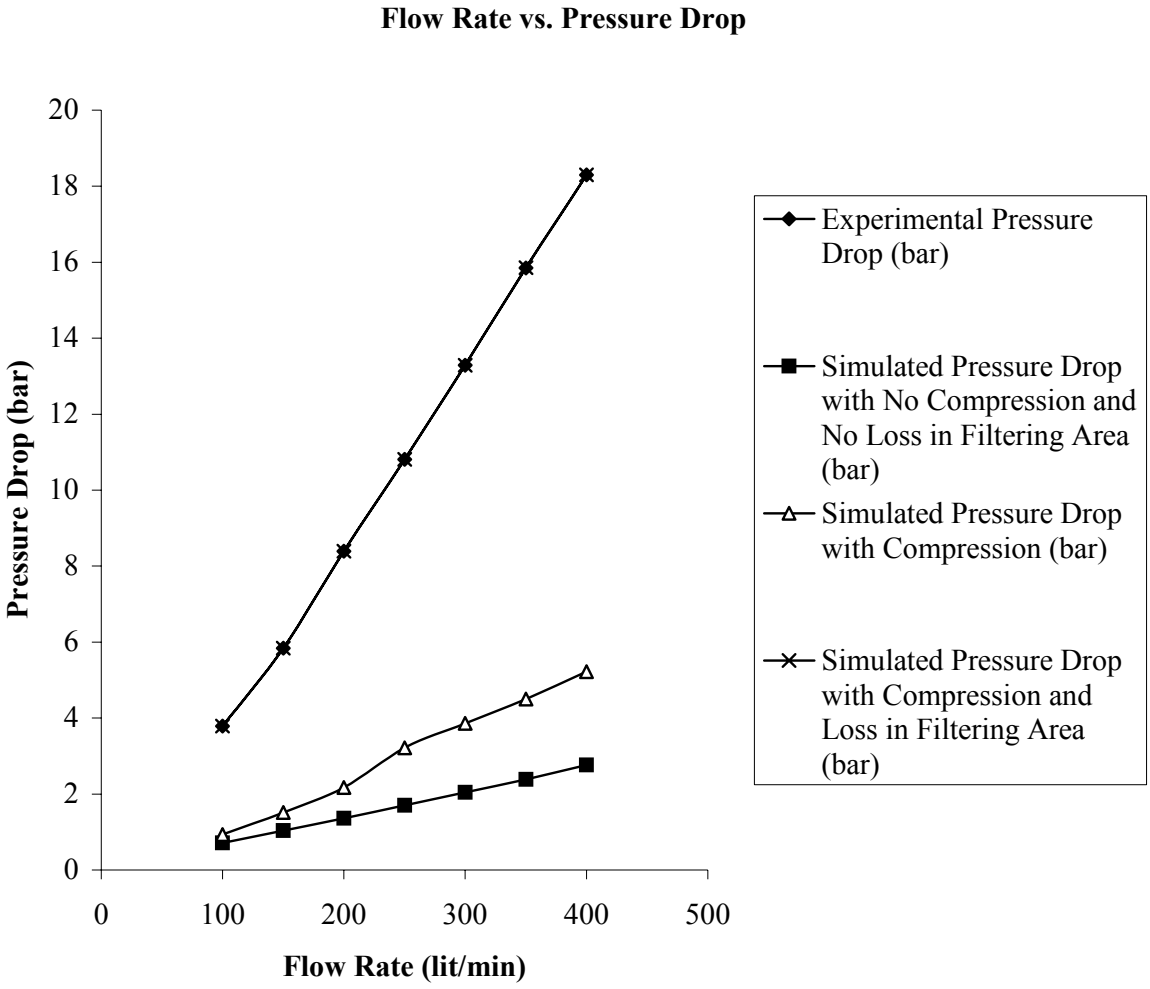

Figure 5 : Validated results for Filter ID 1, flow rate versus pressure drop curve indicates the simulated pressure drops without compression and area loss, with compression and no area loss and with compression and area loss.

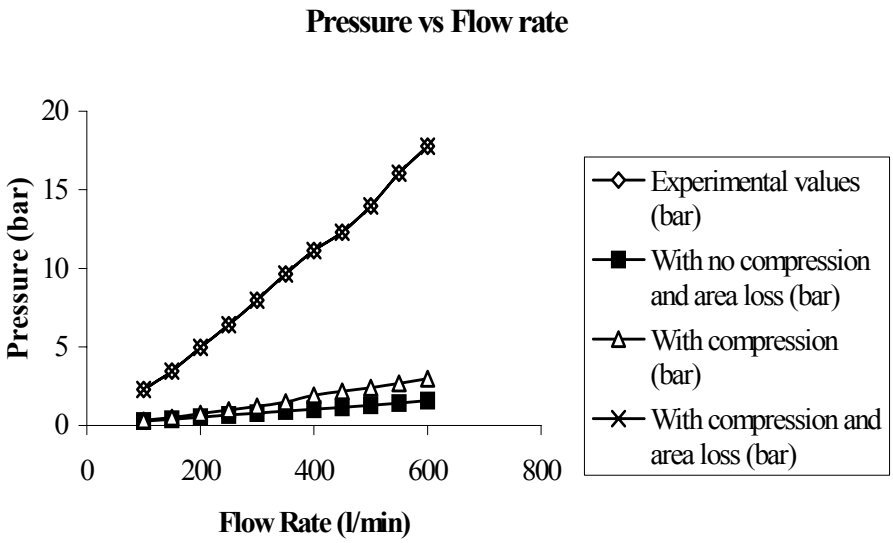

Figure 6 : Validated results for Filter ID 2, flow rate versus pressure drop curve indicates the simulated pressure drops without compression and area loss, with compression and no area loss and with compression and area loss.

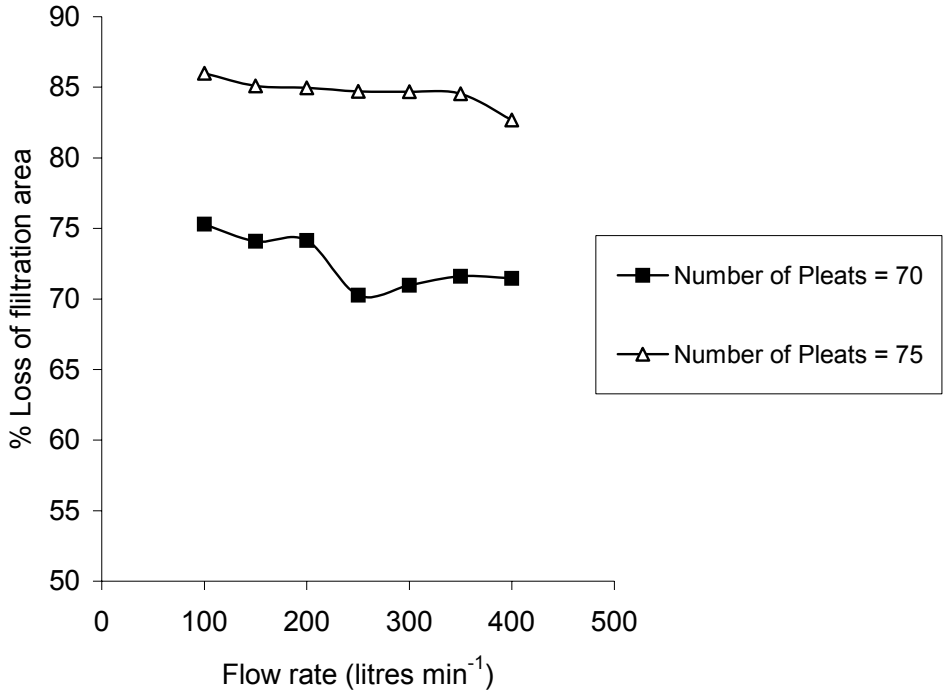

Figure 7: Apparent losses in filtration area increase when the number of pleats id increased from 70 (ID 1) to 75 (ID 2), confirming the pleat crowding effect (length of filter element 211.5 mm, height of pleat 24.5 mm, core diameter 59 mm).

CONCLUSIONS

We have observed in this study that, when losses in area and degree of compression are taken into account, the calculated and experimental pressure drop values for flow through pleated cartridges agree well. The permeability model developed is valid for fibre glass media, however the approach is generic and can be extended for developing models for other media as well. The analysis carried out reveals an optimal design configuration under given test conditions and can be found out using the simulation tool developed by the authors. Significant over-use of media has been illustrated for higher number of pleats and the changes to geometric or mechanical design can be suggested using the procedures described. The authors have suggested modifications in the geometrical designs, which has resulted in an better filtration performance. The developed computer model offers an cost effective, robust and reliable CFD design simulation tool for the engineers in industry for detailed filter analysis.

NOMENCLATURE

c_s	Speed of sound in the fluid, $m.s^{-1}$
K	Permeability of the porous medium, m^2
n	Power law index
p	Pressure, Pa
v	Velocity of the fluid, $m.s^{-1}$
t	Time, s, or uncompressed thickness of the filter medium, m

Greek Symbols

η	Viscosity of the fluid, Pa.s
ρ	Fluid density, $kg.m^{-3}$
η_0	Consistency coefficient used in power law, $Pa.s^n$
$\dot{\gamma}$	Shear rate, s^{-1}
Δp	Pressure drop, Pa
Δx	Thickness of the filter medium, m

Subscripts

exp	Indicates experimental values
c	Indicates compression
c+a	Indicates compression and losses in filtration area
x	Indicates the x-direction
y	Indicates the y-direction

REFERENCES

Hanspal, N.S., Waghode, A.N, Nassehi, V. and Wakeman, R.J., 2004. A Predictive Mathematical Model for Coupled Stokes and Darcy flows in Cross-Flow Membrane Filtration, *54th Canadian Conference in Chemical Engineering,* Calgary, Canada, 3-6 October.

Wakeman, R.J. and Harris, P.R., 1993. A methodology for modelling flow in pleated (star) filter cartridges, *Proc. FILTECH Europa*, Karlsruhe, pp. 335-343, 19-21 October.

Chen, D.R., Pui, D.Y.H. and Liu, Y.H., 1995. Optimisation of pleated filter designs using a finite element numerical model, *Aerosol Science and Technology*, **23**, 579-590.

Oxarango, L., Scmitz, P. and Quintard, M., 2004, Laminar Flow in Channels with Wall Suction or Injection: A New Model to Study Multi-channel Filtration Systems. *Chemical Engineering Science*, **59**, 1039-1051.

Hanspal, N.S., Ruziwa, W.R., Nassehi, V. and Wakeman, R.J., 2004. Finite element modelling of flow of non-Newtonian fluids in pleated cartridge filters, *Proc. 9th World Filtration Congress*, New Orleans Louisiana, USA, Paper 124-3 (CD ROM), 18-22 April.

Waghode, A.N, Hanspal, N.S., Ruziwa, W.R., Nassehi, V. and Wakeman, R.J., 2004. Computational fluid dynamics of free, porous and coupled flows, *Indian Chemical Engineering Journal-Section A*, **46**, 3-6.

Ruziwa, W.R., Hanspal, N.S., Nassehi, V. and Wakeman, R.J., 2003a. Hydrodynamic modelling of pleated cartridge filter media, *Proc. FILTECH EUROPA*, Düsseldorf, Germany, pp. L361-L368, 21–23 October.

Ruziwa, W.R., Hanspal, N.S., Waghode, A.N., Nassehi, V. and Wakeman, R.J., 2004. Computer modelling of pleated cartridge filters for viscous fluids, *Filtration*, **4**, 136-144.

Nassehi, V., 2002. *Practical Aspects of Finite Element Modelling of Polymer Processing*, John Wiley & Sons Ltd., Oxford.

Wakeman, R.J., Hanspal, N. S., Waghode, A.N. and Nassehi, V., 2004 Analysis of Pleat Crowding and Medium Compression in Pleated Cartridge Filters, *IChemE Transactions (submitted)*.

Hanspal, N. S., Waghode, A.N., Nassehi, V. and Wakeman, R.J., 2004. Numerical Analysis of coupled Stokes/Darcy flows in Industrial Filtrations, *Transport in Porous Media Journal (submitted)*.